Determination of the orbital lineup at reactive organic semiconductor interfaces using photoemission spectroscopy

R. Schlaf[a)]
Department of Electrical Engineering, Center for Microelectronics Research, University of South Florida Tampa, Florida 33620

C. D. Merritt,[b)] L. C. Picciolo,[c)] and Z. H. Kafafi[d)]
US Naval Research Laboratory, Code 5615, Washington, DC 20375

(Received 8 January 2001; accepted for publication 2 April 2001)

We determined the orbital lineup of the tris (8-hydroxyquinolinato) gallium (Gaq_3)/Mg interface using combined x-ray and ultraviolet photoemission spectroscopy (XPS and UPS) measurements. The Gaq_3/Mg system is a prototypical model structure for organic electron/low work function electrode transporting materials interfaces found in organic light emitting diodes (OLED). A Gaq_3 thin film was grown in 15 steps on a previously sputter-cleaned Mg substrate starting at a 1 Å nominal thickness up to a final thickness of 512 Å. Before, and in between the growth steps, the sample surface was characterized by XPS and UPS. The results indicate the formation of a reaction layer of about 12 Å thickness at the Mg interface, which resulted in a 0.96 V interface dipole potential. At Gaq_3 coverages higher than 256 Å, a strong charging shift occurred in the overlayer related UPS-emission lines, which was identified by measuring the high binding energy cutoff (secondary edge) of both the XP and UP spectra. The several magnitudes different x-ray and ultraviolet source photon intensities allow pinpointing charging shifts with high sensitivity. Due to the low work function of the reacted interface layer, the Gaq_3 electronic states are aligned at a binding energy below the substrate Fermi edge that exceeds the magnitude of the optical gap between the highest occupied and lowest unoccupied molecular orbitals (HOMO and LUMO). This allowed the conclusion that the ground state exciton binding energy of Gaq_3 needs to be larger than 0.43 eV. Based on these considerations, the lowest possible electron injection barrier matching the experimental data was estimated to be 0.15 eV. © *2001 American Institute of Physics.* [DOI: 10.1063/1.1375016]

I. INTRODUCTION

The demonstration of commercial viability of organic luminescent flat panel displays[1] has recently sparked strong interest in the investigation of the electronic and chemical properties of the interfaces found in organic light emitting diodes (OLEDs). The interfaces between low work function metals and organic electron transport materials have been a major focus of research.[2–7] The need for effective electron injection into the lowest unoccupied molecular orbital (LUMO) demands the use of low work function metal cathodes necessary to achieve low electron injection barriers. The problem with low work function metals such as Mg is that they have a tendency to react with the organic materials. The purpose of this article is to demonstrate a method for the determination of the electronic structure of such reacted interfaces based on our previously established methodology for nonreactive abrupt interfaces.[8–11] In these experiments, it was demonstrated that the use of x-ray photoemission spectroscopy (XPS), in addition to the commonly used ultraviolet photoemission spectroscopy (UPS) measurements, can result in improved accuracy in orbital lineup determinations at organic interfaces. This method is a well-known procedure having been used at inorganic interfaces for many years.[12–15] Therefore in the following evaluation the term ''band bending'' is being used in analogy to measurements at inorganic interface structures in order to explain the XPS core level peak shifts observed in our system with increasing overlayer thickness. It is still unclear whether the source for these peak shifts is really band bending (in a sense of Fermi level equilibration between substrate and overlayer by redistribution of free carriers) or another effect.

In principle, UP spectra contain all the information needed to draw the electronic structure. However, due to the superposition of band bending, interface dipole, highest occupied molecular orbital (HOMO) offset, and possibly charging related shifts on the same spectral features, it is hard to discriminate between these shifts and determine precisely the electronic properties of these interfaces. Additional XPS measurements help disentangle these effects allowing a more meaningful interpretation of the UP-spectral features.

The experiments discussed in this article will demonstrate that XPS can also be used to clarify UPS data obtained on reactive interfaces. Deposition of ultrathin initial overlayers of the organic material in contact with the electrode allows distinguishing between the reaction layer and band

a)Author to whom correspondence should be addressed; electronic mail: schlaf@eng.usf.edu
b)Electronic mail: merritt@ccsalpha2.nrl.navy.mil
c)Electronic mail: crisaful@ccf.nrl.navy.mil
d)Electronic mail: kafafi@ccf.nrl.navy.mil

Report Documentation Page

Form Approved
OMB No. 0704-0188

1. REPORT DATE	2. REPORT TYPE	3. DATES COVERED
2001		**00-00-2001 to 00-00-2001**

4. TITLE AND SUBTITLE	5a. CONTRACT NUMBER
Determination of the orbital lineup at reactive organic semiconductor interfaces using photoemission spectroscopy	5b. GRANT NUMBER
	5c. PROGRAM ELEMENT NUMBER
6. AUTHOR(S)	5d. PROJECT NUMBER
	5e. TASK NUMBER
	5f. WORK UNIT NUMBER
7. PERFORMING ORGANIZATION NAME(S) AND ADDRESS(ES) **Naval Research Laboratory,4555 Overlook Avenue SW,Washington,DC,20375**	8. PERFORMING ORGANIZATION REPORT NUMBER
9. SPONSORING/MONITORING AGENCY NAME(S) AND ADDRESS(ES)	10. SPONSOR/MONITOR'S ACRONYM(S)
	11. SPONSOR/MONITOR'S REPORT NUMBER(S)

12. DISTRIBUTION/AVAILABILITY STATEMENT
Approved for public release; distribution unlimited

13. SUPPLEMENTARY NOTES

14. ABSTRACT

15. SUBJECT TERMS

16. SECURITY CLASSIFICATION OF:			17. LIMITATION OF ABSTRACT	18. NUMBER OF PAGES	19a. NAME OF RESPONSIBLE PERSON
a. REPORT **unclassified**	b. ABSTRACT **unclassified**	c. THIS PAGE **unclassified**		**8**	

bending related peak shifts. The interface under consideration, tris (8-hydroxyquinolinato) gallium (Gaq_3)/Mg, is interesting due to its importance for OLED structures, which are often composed of Mg or Mg/Ag alloys and tris (8-hydroxyquinolinato) aluminum (Alq_3) as a low work function electrode/electron transport layer combination. The optical and electronic properties of Gaq_3 are very similar to Alq_3 while the photoionization cross section of Ga exceeds Al by a factor of 35.7 (Ref. 16) (based on the ratio between Ga $2p_{3/2}$ and Al $2p_{1/2+3/2}$), which is the main reason we used Gaq_3 for these experiments. The large cross section allows for a high signal-to-noise ratio at very thin Gaq_3 coverages. This enables a detailed investigation of the reaction layer and its transition to the nonreacted volume of the interface.

II. EXPERIMENTAL SECTION

The experiments were carried out using a commercial Omicron XP ultrahigh vacuum (UHV) apparatus (background pressure $\sim 5\times10^{-11}$ mbar). The analysis chamber was equipped with an Omicron HIS13 high current UV lamp, a SPECS RQ20/38 x-ray gun, and a VSW EA 125 electron energy analyzer. An interconnected growth chamber holding water-cooled effusion cells (Oxford instruments), a PHI sputter gun, and a Leybold Inficon quartz-crystal thickness monitor (QCM) allowed *in situ* sample preparation and characterization. The base pressure of both chambers was 5×10^{-11} mbar. The effusion cell was controlled by a proportional (PID) controller (Oxford technology) allowing source temperature stability better than ±1 °C. The Mg substrate was prepared by sputtering a 99.999 pure Mg foil for about 24 h with Ar^+ ions (30 mA emission current, 2×10^{-5} mbar Ar pressure in chamber). Before sputtering the Mg foil was heated for 2 h at about 550 °C to remove residual contamination. Gaq_3 was synthesized following a recipe given in Refs. 17 and 18. A detailed description can also be found in Ref. 8.

For the determination of the interface electronic structure, a 512 Å thick (all given thicknesses are nominal as measured with QCM) Gaq_3 film was deposited on the sputter-cleaned Mg substrate in 15 consecutive steps. The deposition rate was 4 Å/min up to a film thickness of 128 Å. The 256 Å growth step was deposited at 10 Å/min and the final step resulting in a 512 Å total coverage was completed using a 15 Å/min rate. The effusion cell temperature ranged from 260 to 275 °C depending on the growth rates. The background pressure during the deposition of the Gaq_3 films was about 1×10^{-9} mbar. After each growth step, the samples were characterized by UPS (He I, 21.21 eV; 1 mm circular entrance slit, 5 eV pass energy) and XPS (Mg $K\alpha$, 12 kV/20 mA). For the measurement of the XP core level spectra, a 6×12 mm slit and 50 eV pass energy were used. The XPS high binding energy cutoff spectra were measured at the same settings used for the UPS measurements. A -5 V bias was applied to the sample during the UPS and XPS high binding energy cutoff measurements in order to distinguish between analyzer and sample cutoffs. XPS high binding energy cutoffs were measured with the x-ray gun retracted by 50 mm from the regular measurement position in order to further reduce the photon flux and minimize the presence of stray electrons photoemitted from the Al bremsstrahlung filter window. The presence of these electrons can result in erroneous work function measurements since they can be drawn into the analyzer nose by the -5 V bias applied during these measurements. In addition, the samples were mounted on a small pedestal elevated about 5 mm from the Omicron standard sample plate. This helped eliminate the collection of stray electrons from the surrounding manipulator/sample plate parts, which can also give rise to an incorrect position of the high binding energy cutoff (HBEC).[8] The spectrometer was calibrated to yield the standard values[19] of 75.13 eV for the Cu $3p$ and 932.66 eV for the Cu $2p(3/2)$ line positions on an Ar^+ sputtered Cu substrate. All given XPS line positions were determined by a fitting procedure described in Ref. 20. The zero binding energy was defined at the Fermi edge position of the sputtered Mg foil. Work function and HOMO cutoff positions were determined from the He I UP spectra by fitting straight lines into the high and low binding energy cutoffs of the spectra and the determination of their intersections with the binding energy axis. In order to determine the work function and the true HOMO cutoff position, these intersection points were corrected for the analyzer broadening which amounts to 0.2 eV.[8] Therefore HOMO cutoff and HBEC binding energy positions were corrected by -0.1 and 0.1, respectively. All data evaluation was carried out using Igor Pro software (Wavemetrics).

III. RESULTS

A 512 Å thick film of Gaq_3 was grown on the previously sputter-cleaned Mg substrate foil in 15 steps. Figure 1 shows the UP spectra obtained before deposition and after each step of the deposition process. The center part of the figure shows the complete spectra while the left graph contains normalized spectra of the HBEC region. The graph on the right shows the HOMO region of the spectra magnified for better comparison. The first spectrum measured on the clean Mg substrate yields a work function of 3.67 eV as determined by the process described in the experimental section. The Fermi edge of the Mg substrate is clearly visible in the right graph and confirms the binding energy calibration of the spectrometer. During the deposition of the first few Gaq_3 layers a strong decrease of the work function (shift of the HBEC to higher binding energy) of the sample surface occurs. This is related to the formation of a reactive interface layer resulting in an interface dipole. At higher coverages the work function increase slows down up to the 256 Å coverage step. The strong shift occurring after deposition of the 512 Å layer is caused by charging phenomena. During the early growth stages, weak Gaq_3 related spectral emissions emerge from the flat Mg s-p-bands related emissions in the 0–12 eV region of the spectra. Particularly notable are the emissions arising in the 0–5 eV range which are distinctively different from undisturbed Gaq_3 layers (compare 256 Å spectrum). At the very beginning two peaks occur which are labeled ''1'' and ''H.'' As the coverage increases the ''H'' peak shifts to higher binding energies and then slightly back while devel-

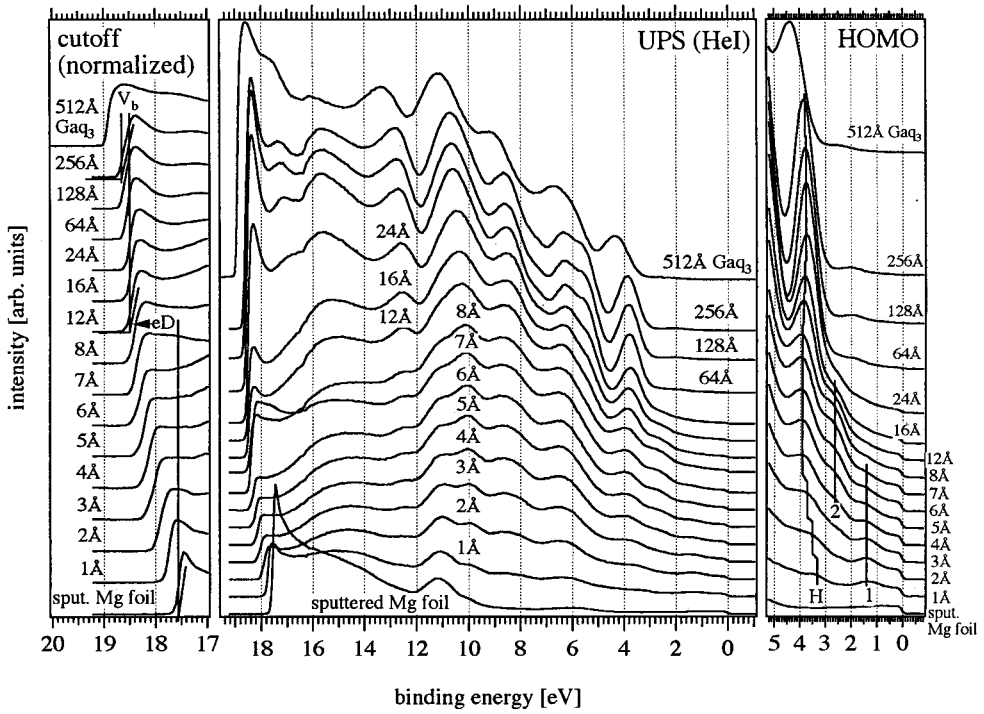

FIG. 1. He I UP spectra of the Gaq_3 film growth sequence. The full spectra are shown in the center part. On the left the high binding energy cutoff (HBEC) regions of the spectra are shown normalized to allow for better comparison. In the top, 12 Å, and bottom spectra the fitted and 0.1 eV shifted (to compensate for the analyzer resolution) lines for the determination of the work function are shown. On the right the development of the peaks of the perturbed Gaq_3 layer (''1,'' ''2'') and the HOMO peak (''H'') with increasing thickness is shown magnified for more detail.

oping into the typical HOMO peak of Gaq_3. The ''1'' peak, on the other hand, remains at its initial position while decreasing in intensity and then vanishes after about 7 to 8 Å Gaq_3 coverage. While peak ''1'' vanishes a new peak, ''2,'' arises at about 4 to 5 Å. This peak also remains at its position and then vanishes at about 16–24 Å coverage. After 24 Å coverage, the typical Gaq_3 related spectral shape establishes itself. The occurrence of the ''1'' and ''2'' peaks indicates the formation of a different chemical species at the interface due to a strong interaction between the Gaq_3 molecules and the Mg surface.

Figure 2 shows the HBEC of the XP spectra. These spectra, while in principal yielding the same information as the UPS HBEC, allow one to pinpoint the onset of charging phenomena in the UP spectra due to the magnitudes weaker x-ray intensity compared to the UV source used for the UPS measurements.[10] As is evident from a comparison between Figs. 1 and 2 the strong shift between the 256 and the 512 Å layers is not apparent in the XPS series indicating that charging artifacts shifted the UP spectrum.

Figures 3 and 4 show the corresponding Ga $2p_{3/2}$ and O $1s$, N $1s$, C $1s$, and Mg $2p$ XPS core level spectra measured along with the UP spectra shown in Fig. 1. The clean substrate shows no emissions in the overlayer related Ga $2p_{3/2}$, N $1s$, C $1s$ regions while showing weak emissions in the O $1s$ region, indicating a small amount of oxide still present after the sputtering process. As the Gaq_3 overlayer grows thicker, the Mg $2p$ emissions become attenuated while the overlayer related peaks strongly increase in intensity. All overlayer related peaks except C $1s$ show two distinctly different peak positions during the first deposited 16–64 Å Gaq_3. This confirms the strong interaction between Gaq_3 molecular species and Mg at the interface.

IV. DISCUSSION

In contrast to our earlier results on Gaq_3 interfaces formed with noble metals [Ag,[8] Au,[9] and Pt Ref. 10], the Gaq_3/Mg interface poses a different challenge for the determination of the interface electronic structure. Since in the noble metal cases strong interface reactions were generally absent, the interface dipole is mainly generated by charge transfer across the interface due to chemisorption or physisorption processes. If strong interface interactions occur, a new (third) phase is created between the two materials in contact which typically results in a ''structural'' or ''chemical'' interface dipole caused by a local polarization due to the interaction or the occurrence of charged defects.[21] The challenge in band line-up measurements at such interfaces is to determine the origin of the spectral shifts observed during the deposition sequence, which can be related to reaction processes in the interaction zone, band bending, or charging occurring in the nonreacted volume regions.

A. Formation of the interfacial interaction layer

The investigated interface offers the benefit of the high photoionization cross section of the Ga $2p$ line allowing well-resolved measurements of the Ga chemical states at submonolayer Gaq_3 coverages. This enables a detailed investigation of the chemical and electronic processes occur-

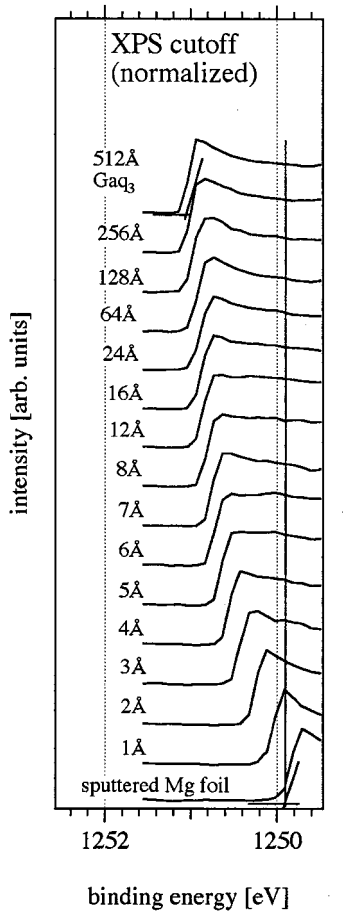

FIG. 2. Normalized XPS high binding energy cutoff (HBEC). The spectra were measured with the x-ray gun retracted in order to minimize the photon flux. This allows the identification of charging phenomena by comparison with the corresponding UP HBECs.

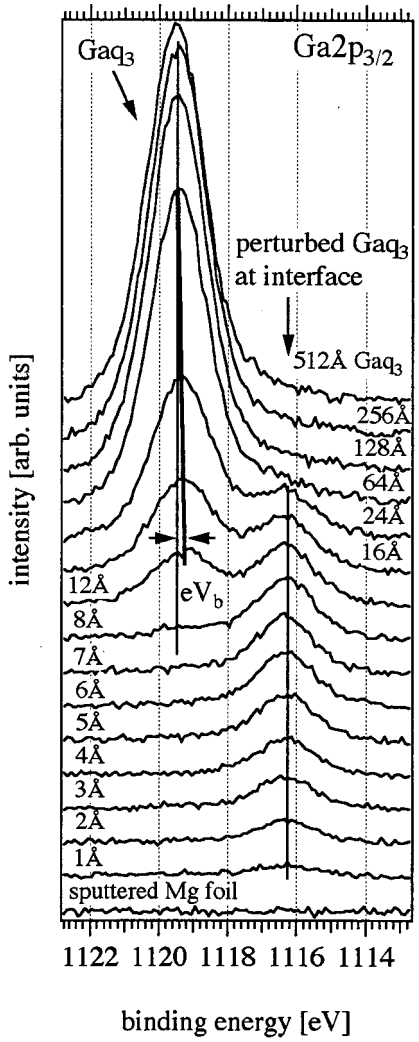

FIG. 3. Evolution of the Ga $2p_{3/2}$ emission line as a function of the Gaq_3 overlayer thickness. The peak developing at 1116.3 eV at low coverages corresponds to the perturbed Gaq_3 layer right at the Mg surface. The line developing at thicker coverages at about 1119.33 eV is related to unperturbed Gaq_3. The slight shift of 0.15 eV to higher binding energies (indicated by the thick line) is a result of developing band bending V_b due to the equilibration of the Fermi levels of Mg substrate and Gaq_3 overlayer.

ring at the interface. The Ga $2p_{3/2}$ spectra sequence in Fig. 3 shows that during the deposition of the first 8 Å of Gaq_3 a distinctly separated peak occurs at 1116.30 eV which is close to the binding energy position known for metallic Ga.[22] As the Gaq_3 layer grows thicker a second peak begins to evolve at 1119.33 eV in the 12 Å spectrum. This peak is related to unperturbed Gaq_3 as can be inferred from previous measurements on noble metals[8–10] where the Ga $2p_{3/2}$ peak occurred in a range between 1117 and 1119 eV depending on overlayer thickness and substrate work function. The occurrence of the thin layer peak is a first indicator for the formation of different Gaq_3 species at the interface. Assuming that 12 Å nominal coverage represents at most two monolayers of Gaq_3, it appears that the molecules in contact with the Mg surface undergo a strong interaction possibly leading to the formation of a metal complex. This is also supported by the occurrence of initially shifted peaks in the corresponding O 1*s* and N 1*s* peaks indicating that the reaction also affects the O and N atoms of the molecule which are bonded to the central Ga atom. In difference to the strongly different initial Ga, O, and N peak positions the C 1*s* peak shows only a relatively weakly shifted position during the first deposition steps. This indicates that the C atoms are not directly partaking in the reaction with the Mg surface.

Comparison of our experimental results with theoretical calculations on Alq_3/metal systems partially supports the above conclusions (Alq_3 has a very similar structure and electronic/optical properties like Gaq_3). The ''1'' and ''2'' peaks observed in the UP spectra (Fig. 1) are in good agreement with calculations performed by Zhang *et al.*[23] In this work it was demonstrated that in a number of possible interactions, scenarios between Mg atoms and Alq_3 peaks appear on the low binding energy side of the HOMO peak. The strong shifts observed in the O 1*s* and N 1*s* emission lines (comp. Fig. 4) in combination with the only weak shifts observed in the C 1*s* peak support the conclusions drawn in Refs. 24 and 25. There it was concluded that mainly the O and N atoms are susceptible to interaction with reducing metals.

From the occurrence of the Ga $2p_{3/2}$ peak related to the unperturbed Gaq_3 species in the XPS data in Fig. 3, the

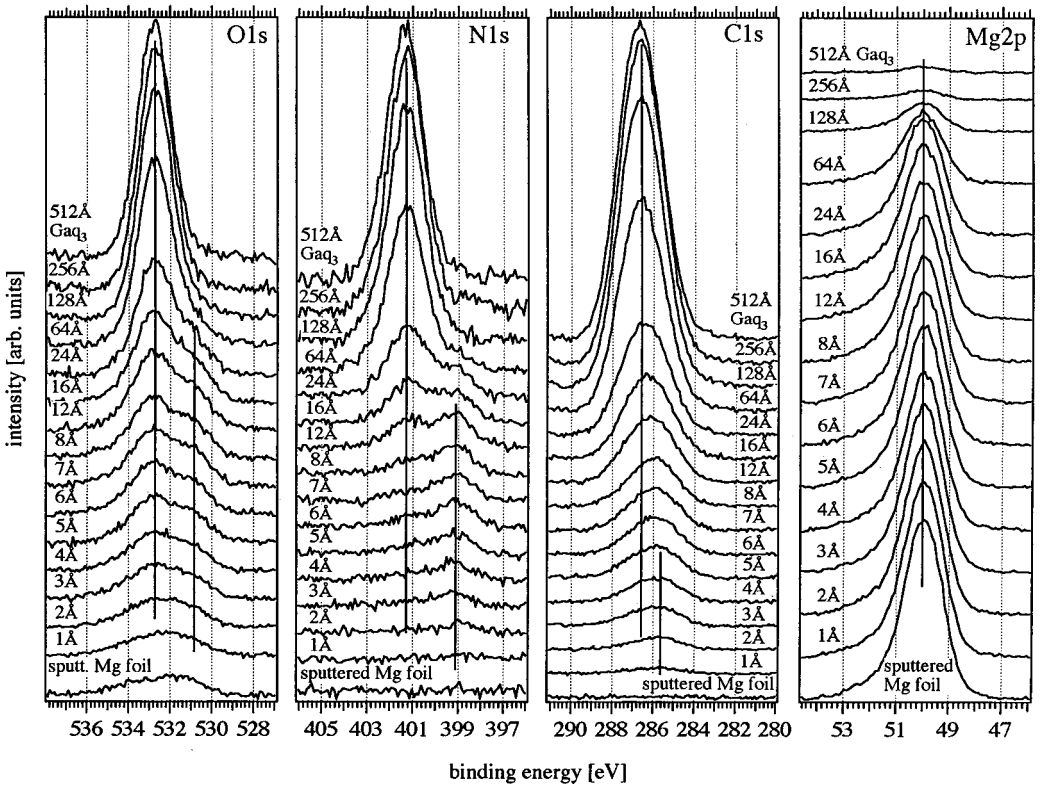

FIG. 4. From left to right: Evolution of the O 1*s*, N 1*s*, C 1*s*, and Mg 2*p* peaks measured parallel to the Ga $2p_{3/2}$ peaks shown in Fig. 3. All Gaq_3 overlayer related peaks (O,N,C) show distinctly shifted line positions at low coverages. These peaks indicate the formation of a perturbed Gaq_3 layer at the interface to the Mg surface.

thickness of the interaction layer was estimated to about 12 Å, corresponding to about 1 to 2 molecular monolayers. The fact that the interaction layer related features in the UP spectra only vanish at about 16–24 Å is related to the approximately 10 Å escape depth that can be assumed for He I excited electrons emitted close to the Fermi edge.[26]

B. Charging effects in the UP spectra

In order to determine the electronic structure of the interface, the onset of charging effects in the UP spectra needs to be determined. This can be done by comparing the thick overlayer shifts of the UPS- and XPS-HBECs shown in Figs. 1 (left graph) and 2, respectively. Comparing the shifts between the 256 and 512 Å deposition steps it is evident that the UPS HBEC shows a fairly strong shift while the XPS HBEC does not shift at all, as is evident from Fig. 5 showing the work function evolution measured by XPS and UPS in comparison. While both XPS and UPS derived values agree very well at coverages below 512 Å, the work function measured by UPS at 512 Å is 0.21 eV smaller than the XPS value. Due to the magnitudes weaker photon flux during XPS measurements we can infer that if both XPS and UPS measurements yield the same value, no charging occurs in either of them. If charging effects begin to play a role they will most likely occur in the UP spectra first due to the much higher photon intensity. Therefore we conclude that the UP spectra of the 256 Å layer can be used to evaluate the electronic structure of the interface.

C. Determination of the electronic structure of the interface

The methodology used in our previous investigations[9–11,27] of nonreactive organic interfaces to determine their electronic structure needs to be extended to

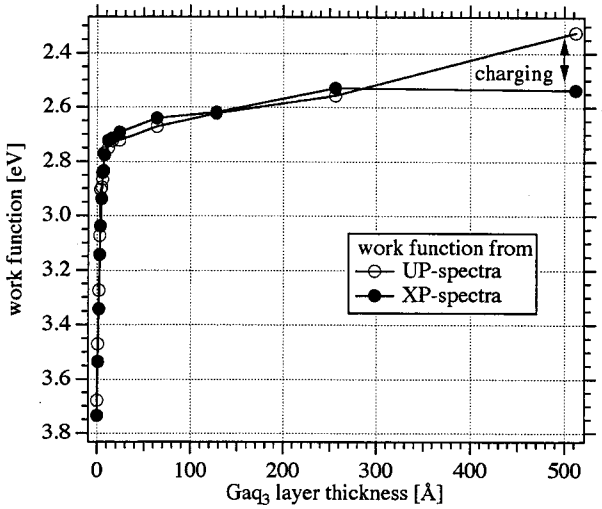

FIG. 5. Comparison between work function values determined from the high binding energy cutoff positions of the XPS and UPS high binding energy cutoff (HBEC) spectra in Figs. 1 and 2. The difference between the values at 512 Å layer thickness is a result from the onset of charging effects due to the low conductivity of the Gaq_3 layer.

account for the interaction layer formed at the interface. The main goal of the measurements is determining the charge carrier injection barriers from the substrate to the overlayer and the magnitude and polarity of the interface dipole.

At nonreactive interfaces the hole injection barrier can be determined with good accuracy by measuring the HOMO position of an overlayer which is thick enough to suppress substrate emissions (hence, showing a well-developed HOMO peak) and still thin enough not to exhibit charging artifacts (to avoid mistakes in the evaluation caused by superimposed charging related shifts). Since the goal is the determination of the HOMO peak right at the interface (=hole injection barrier), the HOMO position determined from the thicker overlayer needs to be corrected for the band bending occurring in the overlayer due to Fermi level equilibration between substrate and overlayer. This can be done by measuring the shift of an overlayer specific core level peak by XPS. Subtraction of the band bending shift yields the HOMO position at the interface. The corresponding LUMO position (=electron injection barrier) can be estimated by using the optical gap of the organic material. The interface dipole can be directly determined by measuring the difference between initial substrate and final overlayer work function and subtracting the band bending determined from the XPS measurements.

At reactive interfaces, this approach needs to be modified to account for the formation of the interaction layer at the interface. The main problem caused by this layer is that it usually changes the work function of the original substrate and, hence, results in a shifted alignment of the electronic states of the unperturbed part of the overlayer relative to the substrate states or Fermi level, respectively. Another problem is determining the band bending likely to occur in the unperturbed part of the overlayer, which grows on top of the interaction layer. Due to the interface reaction most or all core level peaks related to the reaction will be at chemically shifted positions which are usually superimposed to the emission lines of the nonreactive part of the overlayer. This makes it difficult to determine the ''starting point'' of the band bending shift in the unperturbed layer.

In the Mg/Gaq_3 system discussed here, the strong interaction at the interface affects most strongly the Ga atom in the center of the Gaq_3 molecules. The high photoionization cross section of the Ga $2p_{3/2}$ emission line allows one to distinguish effectively between the interaction layer and unperturbed overlayer related Ga $2p_{3/2}$ peaks. Therefore the band bending in the nonreactive overlayer can be obtained from the shift of the Ga $2p_{3/2}$ peak at higher binding energies shown in Fig. 3. From the shift between 12 and 256 Å spectra the band bending eV_b is determined to be 0.15 eV.

The HOMO alignment of the unperturbed layer relative to the Fermi level of the Mg substrate can now be calculated using eV_b and the HOMO position of the 256 Å layer. Figure 6 shows the evaluation of the 256 Å UP spectrum. The top part shows the background determined by using the method described by Li *et al.*[28] The bottom part shows the spectrum after subtraction of the background. The inset contains the HOMO peak region with a Gaussian line shape fitted determining the HOMO maximum position to be at 3.86 eV. The

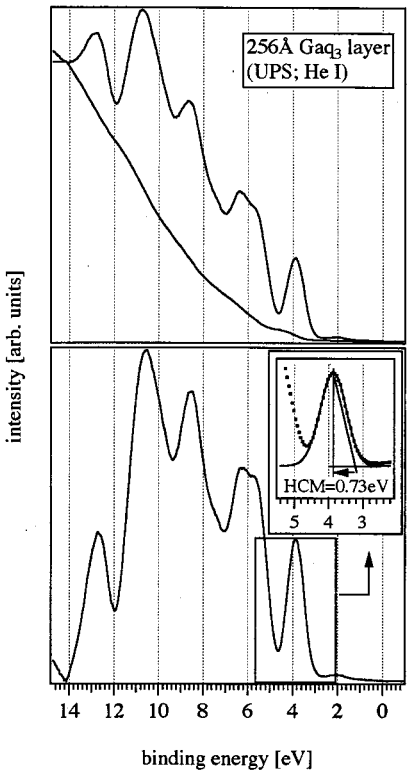

FIG. 6. Background removal procedure and HOMO evaluation of the 256 Å UP spectrum. Top: original spectrum and background signal obtained by fitting the integral of the spectrum into the boundary regions. Bottom: spectrum after background removal. Insert: HOMO of the background removed spectrum fitted with a gaussian and a straight line into the onset of the peak (shown 0.1 eV shifted to account for the analyzer broadening). The difference between the intersection of the line with the zero line and the maximum location of the peak yields the HOMO cutoff to maximum distance (HCM) which was determined to be 0.73 eV.

line drawn on the peak's right side represents the line fitted into the peak flank after shifting it by 0.1 eV to account for the analyzer broadening. The intersection of this line with the base line of the peak represents the ''HOMO cutoff'' position, which was determined to be 3.13 eV. The difference between HOMO cutoff and its maximum (HCM) was calculated to be 0.73 eV, which is consistent with earlier determined values for Gaq_3.[8–10] Subtracting eV_b from the HOMO cutoff position yields 2.98 eV as the HOMO cutoff position (=hole injection barrier Φ_{bh}) at the interface between the perturbed and unperturbed layers relative to the substrate Fermi level.

Using the HOMO-LUMO optical gap of 2.70 eV obtained by optical absorption measurements,[8] the LUMO cutoff alignment relative to the Mg Fermi level can be estimated to be 0.28 eV. In other words the LUMO cutoff right at the interface appears to be below the Fermi level. In fact, at 256 Å, the LUMO cutoff would be located at 0.43 eV below the Fermi level due to the observed band bending of $V_b = 0.15$ eV. If these calculations were correct, the onset of the LUMO peak should be visible in the spectral range between 0 and 0.43 eV in the 256 Å UP spectrum (i.e., the surface would be in deep inversion condition with the Fermi level located in the conduction bands). From Fig. 1 it is evident

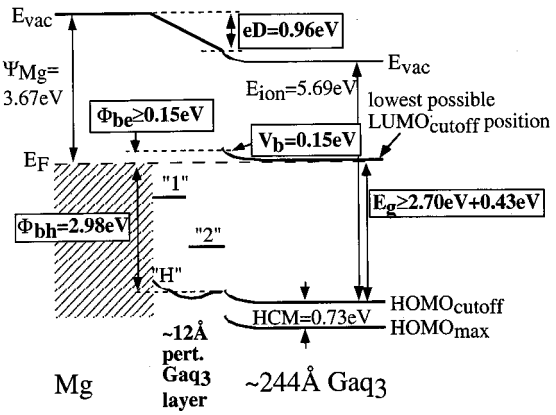

FIG. 7. Electronic structure of the reactive Mg/Gaq_3 interface as determined from the multistep film deposition of Gaq_3 on a sputter-cleaned Mg-foil substrate. The gray shaded area represents the interaction layer estimated to be 12 Å thick. The electronic (interface) states ''1,'' ''2,'' and ''H'' schematically represent the likewise labeled peaks in the UP spectra shown in Fig. 1. The given electron injection barrier estimate of $\Phi \geqslant 0.15$ eV represents a lower limit since the true position of the LUMO is unknown, but must be above the Fermi level at 256 Å coverage.

that there are no such emissions in that spectral range. This indicates that the ground state exciton binding energy of Gaq_3 needs to be at least 0.43 eV allowing to place the LUMO above the Fermi edge, allowing to explain the absence of LUMO emissions in the UP spectra. If we assume the LUMO cutoff is located just above the Fermi level at 256 Å film thickness, we can conclude that the LUMO cutoff to Fermi level electron injection barrier Φ_{be} must be at least 0.15 eV. However, this value can only be regarded as a lower limit for the electron injection barrier since the true exciton energy could surpass the 0.43 eV deducted above resulting in a larger electron injection barrier.

The interface dipole eD comprising the structural/chemical dipole across the perturbed Gaq_3 can be calculated by subtracting eV_b from the total shift of the HBEC between clean substrate and 256 Å overlayer values (we used the UPS HBECs due to their much better signal-to-noise ratio). The work function difference between substrate ($\Psi_{Mg}=3.67$ eV) and 256 Å overlayer (2.56 eV) was determined to be 1.11 eV. Subtracting eV_b yields $eD=0.96$ eV.

Figure 7 shows a schematic of the electronic structure of the interface as determined from our measurements. The perturbed layer was estimated to be about 12 Å leaving 244 Å of the 256 Å totally deposited Gaq_3 to the unperturbed overlayer. The ionization energy $E_{ion}=5.69$ eV of the overlayer was determined by adding the HOMO cutoff to the work function of the 256 Å UP spectrum.

With regard to measurement errors it should be noted that often margins of about ± 0.1 eV are assigned to photoemission measurements. This error margin refers to the determination of the absolute values for ionization energy, work function, and core level peaks. The source of these errors is easily located in the case of the position determination of UP-spectra related cutoff features (HOMO and HBEC). The evaluation of these features strongly depends on the way the lines are fitted into the edges. XPS core level peak positions, however, can be determined very accurately due to the well-defined peak shapes in combination with very precise peak fitting procedures. We estimate that for the case of good signal-to-noise ratio, errors in peak positions can be ± 0.03 eV or better. Therefore the main source of errors in absolute XPS peak positions results more likely from miscalibration of the electron energy analyzers. Since for the determination of orbital offsets, band bending and interface dipole only differences of absolute energy values are used, the errors that have to be considered for these quantities are probably much smaller. This results from the fact that the UPS cutoffs most likely all deviate by the same values since the same evaluation procedure is used for all of them. Also, XPS peaks monitored during a growth sequence will be shifted by the same values throughout the experiment. Therefore we believe that the overall measurement errors in orbital offsets and interface dipoles are in the range of about ± 0.05 eV.

V. CONCLUSION

We prepared a tris (8-hydroxyquinolinato) gallium (Gaq_3)/Mg organic Schottky contact in a multistep deposition of Gaq_3 on a previously sputter-cleaned Mg foil. Before growth and after each growth step the film was characterized by combined x-ray and ultraviolet photoemission spectroscopies (XPS, UPS) allowing the determination of the interface electronic structure. The experiments revealed the formation of an interaction layer of about 12 Å (1 to 2 Gaq_3 monolayers). Our results indicate that the Gaq_3 ligands strongly interact with the Mg surface, giving rise to possibly a Mg:Gaq_3 complex. Using XPS measurements the effects of this interaction layer on the electronic structure of the interface was quantified, yielding electron and hole injection barriers of $\Phi_{be} \geqslant 0.15$ eV and $\Phi_{bh}=2.98$ eV, respectively. The magnitude of the significant interface dipole caused by the interaction layer was determined to be $eD=0.96$ eV. The large value for Φ_{bh} in comparison with the optical gap of Gaq_3 ($E_g=2.70$ eV) allowed the conclusion that the ground state exciton binding energy of Gaq_3 is at least 0.43 eV.

ACKNOWLEDGMENTS

The authors would like to thank the Office of Naval Research and the Petroleum Research Fund for financial support.

[1] J. Burtis, Photonics Spectra, October, 2000, pp. 145.
[2] H. Ishii and K. Seki, IEEE Trans. Electron Devices **44**, 1295 (1997).
[3] H. Ishii, K. Sugiyama, E. Ito, and K. Seki, Adv. Mater. **11**, 605 (1999).
[4] I. G. Hill, A. Rajagopal, A. Kahn, and Y. Hu, Appl. Phys. Lett. **73**, 662 (1998).
[5] I. G. Hill, A. J. Mäkinen, and Z. H. Kafafi, J. Appl. Phys. **88**, 889 (2000).
[6] V.-E. Choong, M. G. Mason, C. W. Tang, and Y. Gao, Appl. Phys. Lett. **72**, 2689 (1998).
[7] Q. T. Le, L. Yan, Y. Gao, M. G. Mason, D. J. Giesen, and C. W. Tang, J. Appl. Phys. **87**, 375 (2000).
[8] R. Schlaf, P. G. Schroeder, M. W. Nelson, B. A. Parkinson, C. D. Merritt, L. A. Crisafulli, H. Murata, and Z. H. Kafafi, Surf. Sci. **450**, 142 (2000).
[9] R. Schlaf, L. A. Crisafulli, H. Murata, C. D. Merritt, Z. H. Kafafi, P. G. Schroeder, M. W. Nelson, B. A. Parkinson, P. A. Lee, K. W. Nebesny, and N. R. Armstrong, Proc. SPIE **3797**, 189 (1999).
[10] R. Schlaf, C. D. Merritt, L. A. Crisafulli, and Z. H. Kafafi, J. Appl. Phys. **86**, 5678 (1999).
[11] R. Schlaf, P. G. Schroeder, M. W. Nelson, B. A. Parkinson, P. A. Lee, K.

W. Nebesny, and N. R. Armstrong, J. Appl. Phys. **86**, 1499 (1999).
[12] K. Horn, Appl. Phys. A: Solids Surf. **51**, 289 (1990).
[13] J. R. Waldrop and R. W. Grant, Phys. Rev. Lett. **43**, 1686 (1979).
[14] R. Schlaf, O. Lang, C. Pettenkofer, W. Jaegermann, and N. R. Armstrong, J. Vac. Sci. Technol. A **15**, 1365 (1997).
[15] R. Schlaf, O. Lang, C. Pettenkofer, and W. Jaegermann, J. Appl. Phys. **85**, 2732 (1999).
[16] J. H. Scofield, J. Electron Spectrosc. Relat. Phenom. **8**, 129 (1976).
[17] F. E. Lytle, D. R. Storey, and M. E. Juricich, Spectrochim. Acta, Part A **29**, 1357 (1973).
[18] H. M. Stevens, Anal. Chim. Acta **20**, 389 (1959).
[19] M. P. Seah, Surf. Interface Anal. **14**, 488 (1989).
[20] I. Kojima and M. Kurahashi, J. Electron Spectrosc. Relat. Phenom. **42**, 177 (1987).
[21] H. Kroemer, in *Molecular Beam Epitaxy and Heterostructures*, edited by L. L. Chang and K. Ploog (Martinus Nijhoff, Dordrecht, 1985).
[22] J. F. Moulder, W. F. Stickle, P. E. Sobol, and K. D. Bomben, *Handbook of X-ray Photoelectron Spectroscopy* (Physical Electronics, Inc., Eden Prairie, MN, 1995).
[23] R. Q. Zhang, X. Y. Hou, and S. T. Lee, Appl. Phys. Lett. **74**, 1612 (1999).
[24] A. Curioni, W. Andreoni, R. Treusch, F. J. Himpsel, E. Haskal, P. Seidler, C. Heske, S. Kakar, T. van Buuren, and L. J. Terminello, Appl. Phys. Lett. **72**, 1575 (1998).
[25] R. Q. Zhang, C. S. Lee, and S. T. Lee, J. Chem. Phys. **112**, 8614 (2000).
[26] W. M. Riggs and M. J. Parker, in *Methods of Surface Analysis*, edited by A. W. Czanderna (Elsevier, Amsterdam, 1975), pp. 103–158.
[27] R. Schlaf, B. A. Parkinson, P. A. Lee, K. W. Nebesny, and N. R. Armstrong, J. Phys. Chem. **103**, 2984 (1999).
[28] X. Li, Z. Zhang, and V. E. Heinrich, J. Electron Spectrosc. Relat. Phenom. **63**, 253 (1993).